Geodesics and BPS States in N=2 Supersymmetric QCD

Jeffrey M. Rabin
Dept. of Mathematics, U.C.S.D.
La Jolla, CA 92093
jrabin@ucsd.edu

September 28, 2006

Abstract

Conformal mapping techniques are used to determine analytically the geodesics on the Seiberg-Witten Riemann surface which correspond to the BPS dyon states in $N = 2$ SUSY QCD with gauge group $SU(2)$ and up to three flavors of massless fundamental matter. The results are exact for zero and two flavors, and approximate in the weak-coupling limit for one and three flavors. The presence of states of magnetic charge 2, in the three-flavor case only, is confirmed.

1 Introduction

The Seiberg-Witten (SW) solution of $N = 2$ supersymmetric Yang-Mills theory with gauge group $SU(2)$ and N_f flavors of fundamental quarks, $0 \leq N_f \leq 3$, is based on assumptions about the spectrum of Bogomol'nyi-Prasad-Sommerfield (BPS) states in this theory, specifically the charges of the particles which become massless at the singularities of the moduli space [1, 2]. These assumptions have been partially checked by several different methods. In the weak-coupling limit, semiclassical and adiabatic arguments lead to a description of the dynamics of slow, heavy dyons in terms of supersymmetric quantum mechanics on the moduli space M_g of monopoles of magnetic charge g [3]. L^2 index theory on M_g provides information about the spectrum of this theory [4, 5]. In particular, the existence of dyons of charge $g = 2$ in the case $N_f = 3$ is demonstrated. However, at present these methods require explicit knowledge of the metric on M_g and the connection on the index bundle of the Dirac operator over M_g. Therefore they are currently limited to charges $g \leq 2$. Arguments based on monodromy at the singularities and the existence of a curve of marginal stability separating weak and strong coupling regions in the moduli space [6, 7] confirm that the SW assumptions are the only consistent ones, but do not directly demonstrate the existence of the assumed dyon states.

Recently, another approach has been developed based on the derivation of the SW description from the low-energy limit of type IIB string theory [8, 9, 10, 11]. The ten-dimensional

string theory is compactified on a Calabi-Yau manifold which is a $K3$ fibration over $\mathbf{P}^1$. This $\mathbf{P}^1$ with its standard complex coordinate z will be denoted $\mathbf{P}^1_z$. The relevant BPS states in this theory are associated with D-branes wrapped around nontrivial 3-cycles of the Calabi-Yau manifold. Their masses are given by the volumes of the cycles as measured by the holomorphic 3-form. At finitely many "branch points" in $\mathbf{P}^1_z$ the $K3$ fibers degenerate by the vanishing of a 2-sphere. The relevant 3-cycles are either $S^2 \times S^1$, where the first factor is in the fiber and the second in the base, or S^3. The latter can be viewed as a singular case of $S^2 \times I$, where the endpoints of the interval I in the base are two of the branch points at which the S^2 vanishes. In the low-energy limit this information about the homology is captured in the SW Riemann surface, which is also a "fibration" (branched cover) of $\mathbf{P}^1_z$. The $K3$ fibers are replaced by discrete sets of points which may be thought of as two endpoints of a diameter of each nontrivial S^2 in the $K3$. Pairs of these points coincide, and sheets of the Riemann surface cross, over the same branch points on $\mathbf{P}^1_z$ where an S^2 vanished. BPS saturated states are D-branes wrapped around minimal volume cycles in their homology classes. This requires that the S^2 be minimal, and then that the S^1 or I be (the image in $\mathbf{P}^1_z$ of) a closed or open geodesic in the SW Riemann surface for a metric induced by the holomorphic 3-form. This (flat) metric turns out to be $|\lambda(z)|^2$, with $\lambda(z)$ the meromorphic differential 1-form of the SW theory. The homology class of the geodesic determines the electric and magnetic charges of the BPS dyon state in the supersymmetric gauge theory. (Strictly speaking, an open curve defines a homology class only relative to its endpoints; reference to the Calabi-Yau setting shows that the charges can be defined by the intersection numbers of the geodesic with a homology basis chosen to avoid the endpoints.)

These geodesics have been computed by numerical integration of the geodesic differential equation for $N_f = 0$ [9], $N_f = 1, 2, 3$ [11], and in some examples from F-theory [12]. In most cases the results confirm the expected BPS spectrum. However, the expected $g = 2$ states for $N_f = 3$ were not found in [11]. An interesting feature of the method is its sensitivity to the 1-form λ itself, not just its periods. We assume in this paper that the 1-form suggested by the integrable systems approach to SW theory [13, 14, 15] is the correct one. This has been partially confirmed by deriving it from string theory for $N_f = 0$ [9] and $N_f = 1$ [16].

In this paper we will describe an analytic method of determining the geodesics based on the conformal mapping to the flat coordinates for the metric, which is just a classical Schwarz-Christoffel mapping. The geodesics of course map to straight lines. For $N_f = 0, 2$ they can be determined exactly at both weak and strong coupling, and the transition can be understood as a change in convexity of the image of the mapping. For $N_f = 1, 3$, they can be described to a good approximation in the weak-coupling limit. The qualitative behavior of the geodesics is easily understood in this framework, including the typical spiral behavior around branch points. The presence of $g = 2$ states for $N_f = 3$ is also clear despite the approximate treatment, although their absence for $N_f = 1$ is less so. The distinction between even and odd N_f is due to the symmetry of the SW curve $F(x, z) = 0$ under $x \to -x$ in the even case. Our discussion is restricted to the case of massless matter.

The SW curve can be viewed as a branched cover of either the z plane ($\mathbf{P}^1_z$) or the x plane ($\mathbf{P}^1_x$). Because the form of λ is simpler and more uniform in N_f when expressed in terms of x, we will generally work in $\mathbf{P}^1_x$. However, it is the z plane which plays the distinguished role as the base of the $K3$ fibration in the derivation from string theory. Thus, the geodesics should join the branch points in $\mathbf{P}^1_z$, even if they are viewed in projection on $\mathbf{P}^1_x$. (This

probably explains the failure of [11] to find the $g = 2$ states.) For $N_f = 0$ we will be able to describe the relation between the projections of the geodesics onto the two planes quite precisely.

In Section 2 we review some conformal mapping techniques, namely the Schwarz-Christoffel mapping and the Schwarz reflection principle. Section 3 recaps the SW curves for various N_f, their branch points in both the x and z planes, and the differentials λ.

Section 4 treats the cases of even N_f. The Schwarz-Christoffel mapping gives a simple and exact description of the image of the x plane for real values of the moduli space coordinate u. For $N_f = 0$ we describe the geodesics in both weak- and strong-coupling limits, and the transition between these. The explicit mapping between the x and z planes is also described. $N_f = 2$ exhibits the new feature arising from the presence of matter: the opening of a "window" between the right and left half x planes. Because of the positioning of the branch points, it is not exploited in this case, however. Still, we make use of the exact solution of this case to draw lessons about the behavior of the geodesics in such regions which can be applied to the remaining cases with matter.

Section 5 discusses the cases $N_f = 1, 3$. These differ in the positioning of the branch points in relation to the window. Unfortunately we cannot identify any convenient region of the left x plane whose image is bounded by straight line segments to which the Schwarz reflection principle applies. Therefore our treatment of the geodesics is less complete. However, we can say enough about their behavior to argue for the presence of the $g = 2$ dyon states for $N_f = 3$.

Section 6 contains some concluding remarks.

As this paper was being completed, additional works appeared in which analytic methods for determining the geodesics were proposed [17, 18].

2 Geodesics and Conformal Mapping

The metric $|\lambda(x)|^2$ induced by the SW differential on $\mathbf{P}^1_x$ is flat; one can go to flat coordinates w by the conformal mapping $dw = \lambda(x)$ or

$$w = \int^x \lambda(x). \tag{1}$$

In all cases of interest here λ has the form

$$\lambda(x) = \prod_i (x - x_i)^{\alpha_i} dx, \tag{2}$$

exhibiting zeros and branch points at the various x_i. Such a conformal map is an example of a Schwarz-Christoffel mapping [19]. In our cases we will always have $\sum_i \alpha_i = 0$, so that the map approaches the identity for large x. The image of a straight line under such a map can be determined by writing

$$\arg dw = \arg dx + \sum_i \alpha_i \arg(x - x_i). \tag{3}$$

As x moves along the line, w moves along a curve whose direction is locally given by $\arg dw$, hence determined by the variation of the $\arg(x - x_i)$. If, in particular, the x_i are all real and we ask for the image of the real axis, then $\arg dw$ is piecewise constant, changing by $-\pi\alpha_i$ as x passes x_i from left to right. The image consists of straight line segments joining the images of the x_i. The image of the upper half plane lies to the left of this polygonal path. We will apply these ideas to slightly more general regions, namely quadrants.

We recall also the Schwarz reflection principle [19]. This describes the analytic continuation of a conformal mapping across a straight line segment in the domain whose image is also straight. In the above context, if x passes from the upper to the lower half plane across a segment of the real axis, the image point passes from the image of the upper half plane into a region which is its reflection across the particular boundary segment which is crossed. The distinct regions resulting from reflection across different segments display the monodromy properties of the mapping around the branch points.

3 The Curves

The hyperelliptic curves describing $N = 2$ SUSY $SU(2)$ QCD with N_f flavors of massless matter are given by [13, 20]

$$z + \frac{Q(x)}{z} = 2P(x), \tag{4}$$

where $Q(x) = \Lambda^{4-N_f} x^{N_f}$ and

$$\begin{aligned} P(x) &= x^2 - u, && N_f = 0, 1. \\ P(x) &= x^2 - u + \frac{\Lambda^2}{8}, && N_f = 2. \\ P(x) &= x^2 - u + \frac{\Lambda}{4}x, && N_f = 3. \end{aligned} \tag{5}$$

Λ is the dynamically generated scale and the moduli space is the complex u plane. In the weak-coupling limit $u \to \infty$ which will be our main concern we can take $P(x) = x^2 - u$ in all cases. We will always consider real positive values of u. We will also set $\Lambda = 1$. The change of variables

$$y = z - P(x) = \frac{1}{2}[z - \frac{Q(x)}{z}] \tag{6}$$

brings the curves to the standard hyperelliptic form

$$y^2 = P(x)^2 - Q(x). \tag{7}$$

The polynomial $P(x)^2 = (x^2 - u)^2$ has, of course, two double zeros at $x = \pm\sqrt{u}$. For N_f even, the perturbation $-Q(x) = -x^{N_f}$ is negative at each zero and therefore splits the double roots into two pairs of real roots given for large u by

$$\pm u^{1/2} \pm \frac{1}{2}u^{(N_f-2)/4}, \tag{8}$$

with the two signs chosen independently. These two pairs of branch points in the x plane are related by the symmetry under $x \to -x$. This symmetry is absent for N_f odd, and indeed the perturbation is then positive at $x = -\sqrt{u}$, which therefore splits into a pair of *complex* branch points,

$$-u^{1/2} \pm \frac{i}{2} u^{(N_f-2)/4}, \tag{9}$$

while the positive root still splits as above.

Within the framework of supersymmetric gauge theory, the Seiberg-Witten differential λ is not determined within its cohomology class. However, both the integrable systems approach [13, 15] and the derivations via the low-energy limit of string theory [9, 16] suggest the specific representative

$$\lambda = x \, d \log \frac{z}{\sqrt{Q(x)}} = \frac{dx}{y} \frac{2QP' - PQ'}{2Q}. \tag{10}$$

For our curves in the weak-coupling limit we find

$$\lambda = \frac{x \, dz}{z} - \frac{N_f}{2} dx = \frac{dx}{2y}[(4 - N_f)x^2 + N_f u], \tag{11}$$

although we will choose the normalization

$$\lambda = \frac{dx}{y} \left(x^2 + \frac{N_f}{4 - N_f} u \right). \tag{12}$$

Note the pair of zeros on the imaginary axis at $x = \pm i \sqrt{\frac{N_f}{4-N_f} u}$ in addition to the branch points at the above zeros of y.

Generically, a distance measured by the metric λ is of the same order as the coordinate distance in the x plane, the basic scale being set by $\sqrt{u}$. However, distances are increased near branch points of λ, e.g. by $\log u$ factors, and decreased near its zeros.

We will also need the (finite) branch points in $\mathbf{P}^1_z$, the endpoints of the relevant geodesics. These are the points z at which

$$z + \frac{x^{N_f}}{z} = 2(x^2 - u) \tag{13}$$

has fewer than the generic number of solutions for x. For $N_f < 3$ this generic number is two, and by the $x \to -x$ symmetry the branch points must occur for $x = 0$ when N_f is even. For $N_f = 0$ we find

$$z = e_\pm = -u \pm \sqrt{u^2 - 1}, \tag{14}$$

or, at weak coupling, $e_- = -2u$ and $e_+ = -1/2u$. For $N_f = 2$ we have simply $e_- = -2u$, $e_+ = 0$.

For $N_f = 1$ the solution for x is

$$x = \frac{1}{4} \left[z^{-1} \pm \sqrt{z^{-2} - 8(z + 2u)} \right]. \tag{15}$$

The branch points are the roots of a cubic equation and for large u are given by

$$\begin{aligned} z &= -2u \qquad\qquad (x = -1/8u), \\ z &= \pm\frac{1}{4\sqrt{u}} - \frac{1}{64u^2} \qquad (x = \pm\sqrt{u} + \frac{1}{16u}). \end{aligned} \tag{16}$$

For $N_f = 3$ the generic number of solutions for x is three, and there are branch points at which generically pairs of these coincide. They are the zeros of the discriminant Δ of the cubic

$$x^3 - 2zx^2 + z(z+2u) = 0, \tag{17}$$

namely

$$\Delta = \frac{1}{4}z^2(z+2u)\left[(z+2u) - \frac{32}{27}z^2\right]. \tag{18}$$

The branch points are at $z = 0$, corresponding to $x = 0$; $z = -2u$, corresponding to $x = -4u$ and $x = 0$; and the roots of the quadratic, which are approximately

$$z = \pm\frac{3\sqrt{3}}{4}\sqrt{u} \quad (x = \pm\sqrt{3u},\ \mp\frac{\sqrt{3}}{2}\sqrt{u}). \tag{19}$$

4 The Cases $N_f = 0, 2$

The SW curve for $N_f = 0$ is $z + z^{-1} = 2(x^2 - u)$, or $y^2 = (x^2 - u)^2 - 1$, and the conformal mapping which flattens the metric on the x plane is

$$w = \int^x \frac{x^2\,dx}{\sqrt{(x^2-u)^2 - 1}}. \tag{20}$$

The double zero of $\lambda(x)$ at the origin causes the map to locally triple angles there, so the map is not one-to-one on the upper half-plane. Therefore it is convenient to study the image of a quadrant instead. Figure 1 shows the image of the first quadrant and some of its Schwarz reflections representing the fourth quadrant for weak coupling, $u >> 1$. (All figures in this paper show qualitative behavior correctly, but are not necessarily strictly to scale.) The image of the imaginary axis is a straight line thanks to the symmetric placement of the branch points, which causes the changes in the $\arg(x - x_i)$ to cancel as x moves down this axis. Reflecting across the imaginary axis, we see that the images of the first and second quadrants overlap in a rectangle, which is the region covered twice in mapping the entire upper half-plane. The sides of this rectangle are the SW half-periods, $\frac{\pi}{2}\sqrt{u}$ (vertical) and $\sqrt{u}\log u$ (horizontal). The geodesics we seek are straight lines from $x = 0$ (the image of both branch points in $\mathbf{P}^1_z$) to one of its reflected images. Such geodesics can meet the branch cut joining the branch points on the positive real axis at most once (at an endpoint), corresponding to the magnetic charge, but by passing through many reflected regions may cross the rest of the positive real axis an arbitrary number of times, giving arbitrary electric charge. In the x plane, these geodesics are somewhat singular: they leave $x = 0$, spiral around the cut until

they reach one of its endpoints, and then retrace the same path backwards to $x = 0$. By the $x \to -x$ symmetry there are similar geodesics in the left half-plane, but none which cross the imaginary axis. A small change in the initial direction produces a geodesic which loops around the endpoint of the cut rather than terminating there, follows almost the same path backwards, turns around just short of $x = 0$ and runs out to infinity.

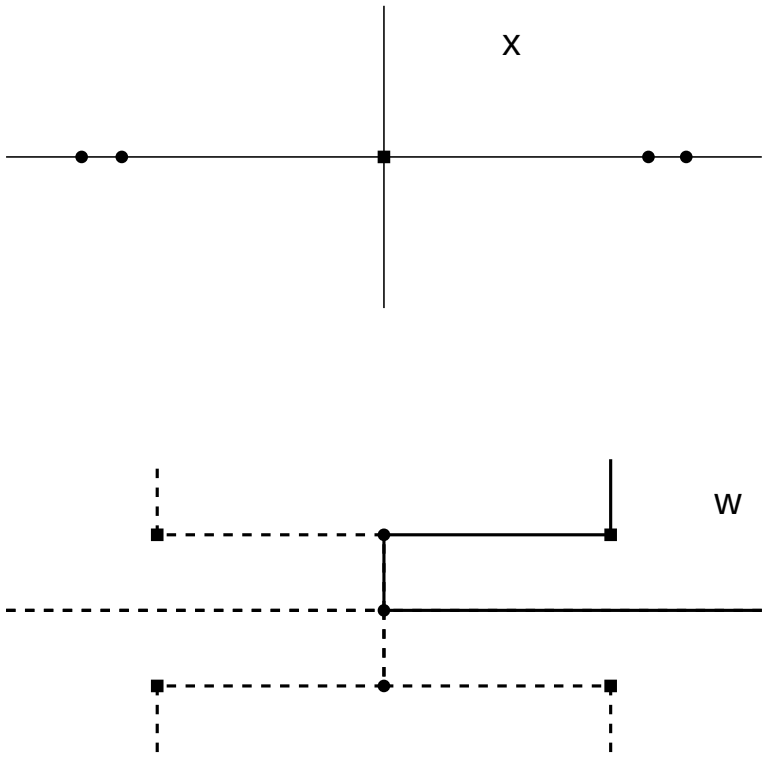

Figure 1: The image of the first quadrant in the x plane lies to the right of the solid boundary in the w plane. Branch points on $\mathbf{P}^1_x$ are labelled by dots, those on $\mathbf{P}^1_z$ by squares. Reflections of this region across segments of the positive real axis are also shown. Straight lines joining the squares acrue one unit of magnetic (electric) charge in crossing a vertical (horizontal) boundary between regions.

Due to the simplicity of this case we can trace the geodesics back to the "physical" z plane. Introduce an intermediate s plane by

$$z + \frac{1}{z} = 2s = 2(x^2 - u). \tag{21}$$

The map from x to s doubles angles to expand the right x plane to the entire s plane, sending the origin to the point $s = -u$ and the branch cut to $[-1, 1]$. The map from z to s is a standard Joukowski transformation sending the exterior as well as the interior of the unit circle to the cut s plane. The branch points e_-, e_+ in the z plane lie in the exterior and interior of the circle, respectively. The $g = 1$ geodesics which met the cut now cross this circle and indeed join e_- with e_+, while the $g = 0$ geodesics are now closed curves with both endpoints at, say, e_-, as expected for the gauge bosons. These mappings are illustrated in Figure 2.

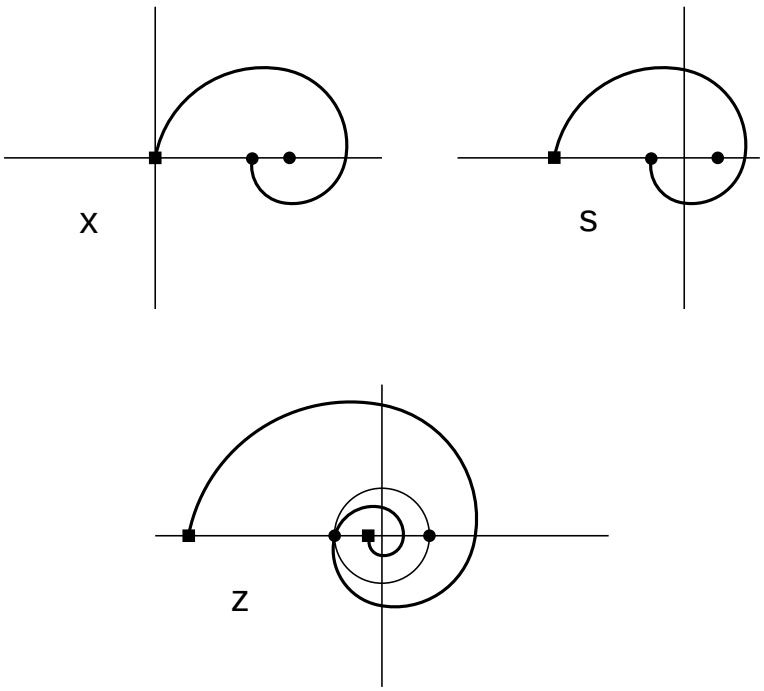

Figure 2: Views of a $(g, q) = (1, 2)$ geodesic in the x, s, and z planes.

We can also study the conformal mapping of the x plane in the strong-coupling case $0 < u < 1$ and understand the transition as u crosses $x = 1$, where the curve of marginal stability meets the real axis. As u decreases, the branch points on $\mathbf{P}^1_x$ move toward the origin. When $u = 1$ the inner pair of branch points meet there, and the homology cycle encircling this pair vanishes. As u decreases further these points separate along the imaginary axis, leaving one branch point on each half axis at strong coupling. In this process the homology cycle dual to the vanishing cycle is shifted by half its Picard-Lefschetz monodromy around the singularity. Figure 3 shows the image of the first quadrant in this case. Due to the change in convexity of the image region, the only straight lines from $x = 0$ to an image point which remain in the region are now the vertical and horizontal lines. These would represent pure electric or magnetic charges if not for the change in the homology basis which occurs in passing the singular point $u = 1$ [6]. In fact they correspond to the weak coupling states $(g, q) = (0, 1), (1, 1)$. We have thus understood completely the representation of BPS states by geodesics in this case.

The two-flavor case is very similar. We treat only the weak-coupling limit. The curve still has the $x \to -x$ symmetry which leads to a symmetric placement of branch points in $\mathbf{P}^1_x$ and puts both of the $\mathbf{P}^1_z$ branch points at $x = 0$. The major change in the mapping,

$$w = \int^x \frac{(x^2 + u)\, dx}{\sqrt{(x^2 - u)^2 - x^2}}, \tag{22}$$

is that the double zero of $\lambda(x)$ at the origin has split into two zeros on the imaginary axis. Figure 4 shows the resulting image of the first quadrant. The part of the imaginary axis between the origin and the new zero is mapped to a small "window" which can be crossed

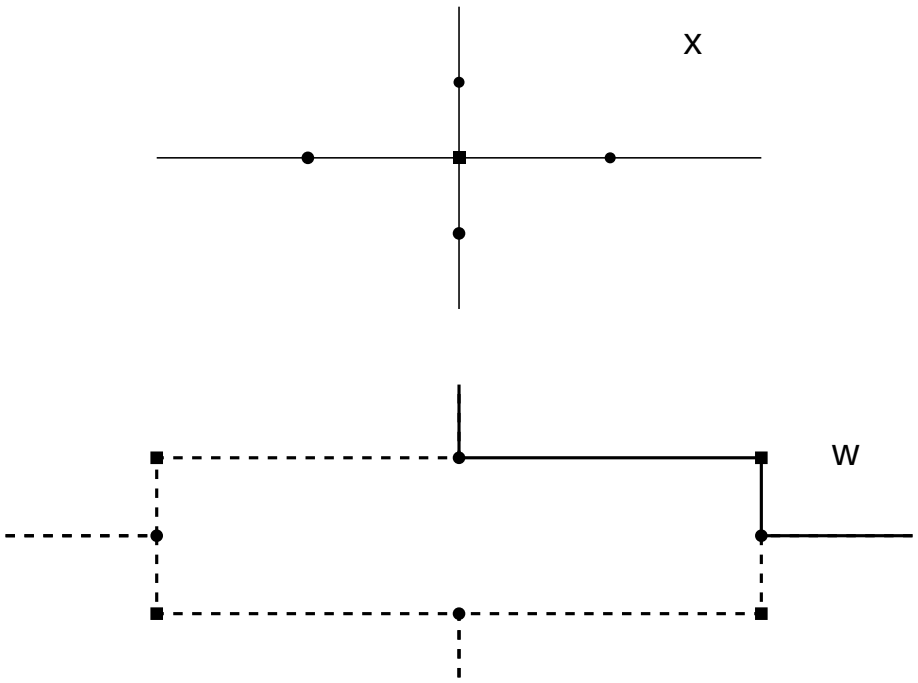

Figure 3: For strong coupling the image of the first quadrant together with some of its reflections forms the exterior of the rectangular region shown. Straight lines joining the branch point images cannot enter the rectangle and must lie on its boundary.

from left to right, leading by reflection into an image of the second quadrant. However, the geodesics which start and end at $x = 0$ cannot take advantage of this possibility, and behave just as for $N_f = 0$, as expected. (A geodesic which starts at $x = 0$ and passes through the window may spiral around $x = 0$ but will eventually run out to infinity.) The existence of the window will persist in the odd N_f cases which are not exactly solvable by our methods. Its size is $O(\sqrt{u})$ but the numerical coefficient grows with N_f. (Its size relative to the vertical segment in the w plane which is the image of the branch cut is 6%, 18%, and 39% in the cases $N_f = 1, 2, 3$ respectively.) Therefore, let us study the qualitative behavior of other geodesics in the present case, to develop intuition which will apply more generally. A geodesic which crosses the cut at a very small angle will then pass through many reflected regions in the vertical direction, meaning that it spirals outward around the cut many times. If it misses the window it will run out to infinity. If it passes through the window it enters the left half-plane and spirals inward toward the cut there, eventually crossing that cut. It then begins spiraling outward and the behavior repeats. Very small changes in the initial direction of the geodesic can make it pass through any desired point on the real axis, and hit or miss the window. Increasing the angle at which the geodesic crosses the cut decreases the number of spirals and thus the electric charge. At weak coupling the cuts are well separated from each other and from other features such as zeros, so the local spiraling behavior around the cuts should occur in all cases independent of other global differences.

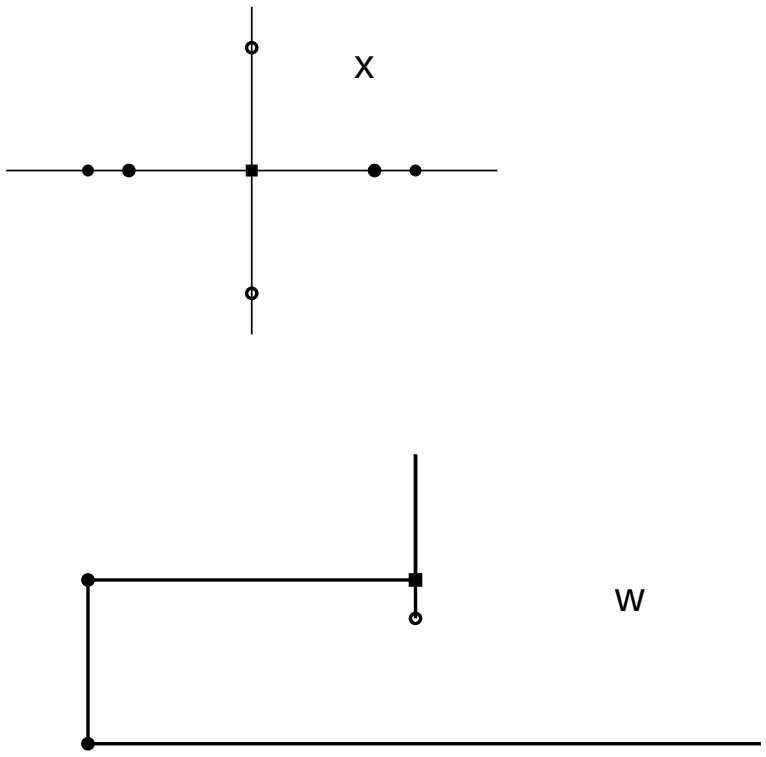

Figure 4: The image of the first quadrant for $N_f = 2$. Open circles mark zeros of the SW differential λ, which produce a small "window" in the image. Straight lines joining the squares to their reflected images do not pass through this window but duplicate the behavior for $N_f = 0$.

5 The Cases $N_f = 1, 3$

When N_f is odd we lose the $x \to -x$ symmetry. The branch points in $\mathbf{P}^1_x$ form a real pair near $\sqrt{u}$ and a complex conjugate pair near $-\sqrt{u}$. At weak coupling the separation between the pairs is large while the splitting within each pair is small (absolutely so for $N_f = 1$, relatively so for $N_f = 3$). The image of the imaginary axis under the conformal mapping is not exactly straight due to the imperfect cancellation between the $\arg(x - x_i)$ contributions of the pairs of branch points, but this effect is small. More consequentially, the image of the line L through the pair of complex branch points is not straight due to the $\arg(x - x_i)$ contributions from the zeros on the imaginary axis and the distant pair of branch points. Figure 5 shows the images of the first quadrant and a region in the second quadrant bounded by the real and imaginary axes and L. The important feature is the placement of the branch points from $\mathbf{P}^1_z$ in the image. One lies on the branch cut near $\sqrt{u}$, one very near $(O(u^{-1}))$ the origin, and one very near $(O(u^{-1/4}))$ the center of the cut near $-\sqrt{u}$. Although we cannot use Schwarz reflection for the lines that are not straight, it should be approximately valid where they are nearly so. Further, the local spiral behavior of the geodesics near the branch points is universal. Geodesics leaving the "positive" branch point cross the homology generator encircling the cut, which contributes 1 to the magnetic charge. To obtain a state

with magnetic charge 2, such a geodesic would have to pass through the window, cross the cut near $-\sqrt{u}$, and end at the "negative" branch point. The positioning of the negative branch point very near the cut makes it quite hard to hit. It requires that the image of the geodesic be a nearly vertical line which passes through many reflected regions before crossing the window. However, it then enters the second (or third) quadrant and crosses the line L far from the branch points, where the reflection principle does not apply. We conclude cautiously that there is no evidence for states of magnetic charge 2 in the one-flavor theory, although charges 0 and 1 exist.

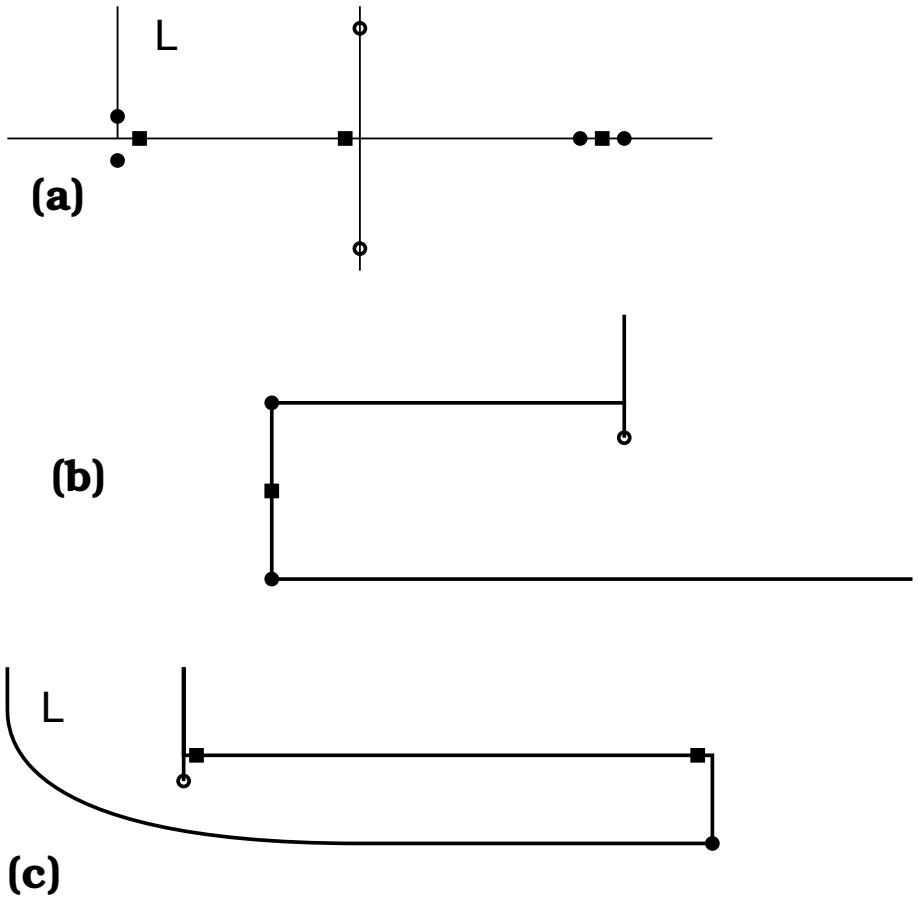

Figure 5: The case $N_f = 1$. The x plane (a) is shown, along with the images of the first quadrant (b) and the semi-infinite rectangle in the second quadrant (c). A line entering (c) through the window, crossing the distant cut, and ending on the reflection of the nearby square across it would have to have slope of order $u^{3/4}$, and would have met the curved portion of L.

The placement of the branch points for $N_f = 3$ is quite different, as shown in Figure 6. Most branch points have two images in $\mathbf{P}^1_x$, and their locations are more generic in that they are not unnaturally close to branch cuts. This allows them to be connected by lines whose slopes are not unnaturally large. In addition to a variety of $g = 0, 1$ states, there are now geodesics which leave one of the branch points on the positive real axis, cross the

cut there, pass through the (larger) window, cross the cut in the left half-plane and spiral around it until they end on a branch point there, crossing boundaries only where they are straight to a good approximation. Therefore the existence of these geodesics seems reliable despite the approximation. In terms of the qualitative behavior of geodesics gleaned from the $N_f = 2$ case, given that geodesics exist which cross both cuts, small perturbations suffice to make them pass through arbitrary points not too far away, including the desired branch endpoints.

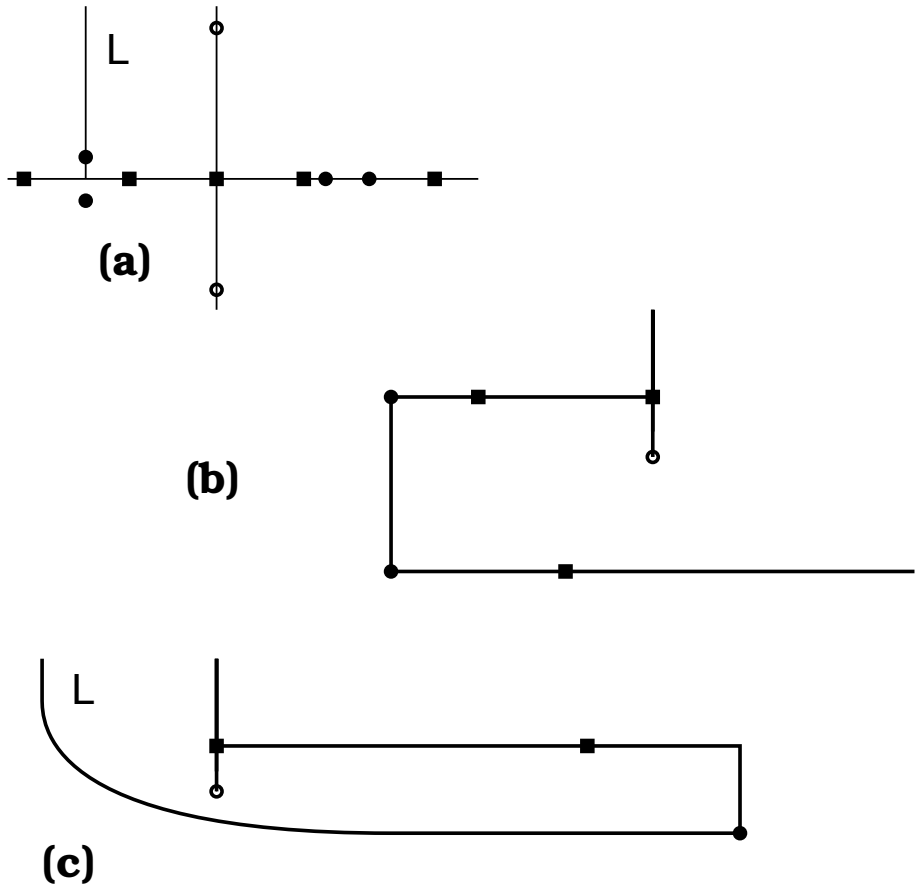

Figure 6: The case $N_f = 3$. The x plane (a) and images of the first quadrant (b) and the semi-infinite rectangle in the second quadrant (c). In contrast to $N_f = 1$, lines having slope of order 1 can cross the cuts in both quadrants to join branch points.

6 Conclusions

We have used simple conformal mapping techniques to determine the geodesics corresponding to the BPS states of $N = 2$ supersymmetric QCD with gauge group $SU(2)$, exactly for even N_f and approximately at weak coupling for odd N_f. Qualitative features of the geodesics such as the typical spiral behavior around branch cuts become transparent in this approach. The important changes as N_f is increased involve the placement of the branch points on $\mathbf{P}^1_z$

relative to those on $\mathbf{P}^1_x$. The transition between weak and strong coupling involves a change in convexity of the image region, which obviously alters the set of straight lines which can connect boundary points. Although we considered only real positive values of u, for which the classical Schwarz-Christoffel mapping applies, even when u is complex the convexity of the image region can only change upon crossing the curve of marginal stability. Indeed, the arguments of [6, 7] concerning the spectrum outside and inside this curve could be directly rephrased as arguments about the behavior of the geodesics in these regions.

In our treatment it is quite clear that for $N_f = 0, 2$ the maximum magnetic charge of an elementary BPS state is 1. For N_f odd the maximum charge is 2. Such states seem to exist for $N_f = 3$ due to the "generic" placement of the branch points, which allows them to be connected by straight lines without unnatural "fine-tuning". For $N_f = 1$, fine-tuning would be necessary to obtain such states but our approximations are not reliable for such fine-tuned lines. No such states are found in numerical studies [11].

These methods should be applicable to $N = 2$ theories with other gauge groups, possibly with massive matter. The main requirement is that there exist a region of the moduli space in which all branch points on $\mathbf{P}^1_x$ are real, or nearly so. Symmetries relating the branch points are also very useful. One may hope that with analytic understanding of the geodesic description of BPS states will come an understanding of the relation between this description and that of L^2 index theory.

Acknowledgements

I have enjoyed discussions with Albrecht Klemm, Harold Stark, Nicholas Warner and Eric Zaslow.

References

[1] N. Seiberg and E. Witten, "Electric-magnetic duality, monopole condensation, and confinement in $N = 2$ supersymmetric Yang-Mills theory," Nucl. Phys. **B426** (1994) 19–52; **B430** (1994) 485–486 (E), hep-th/9407087.

[2] N. Seiberg and E. Witten, "Monopoles, duality and chiral symmetry breaking in $N = 2$ supersymmetric QCD," Nucl. Phys. **B431** (1994) 484–550, hep-th/9408099.

[3] J. P. Gauntlett, "Low-energy dynamics of $N = 2$ supersymmetric monopoles," Nucl. Phys. **B411** (1994) 443–460, hep-th/9305068.

[4] S. Sethi, M. Stern, and E. Zaslow, "Monopole and dyon bound states in $N = 2$ supersymmetric Yang-Mills theories," Nucl. Phys. **B457** (1995) 484–510, hep-th/9508117.

[5] J.P. Gauntlett and J.A. Harvey, "S-duality and the dyon spectrum in $N = 2$ super Yang-Mills theory," Nucl. Phys. **B463** (1996) 287–314, hep-th/9508156.

[6] F. Ferrari and A. Bilal, "The strong-coupling spectrum of the Seiberg-Witten theory," Nucl. Phys. **B469** (1996) 387–402, hep-th/9602082.

[7] A. Bilal and F. Ferrari, "Curves of marginal stability, and weak and strong coupling spectra in $N = 2$ supersymmetric QCD," Nucl. Phys. **B480** (1996) 589–622, hep-th/9605101.

[8] S. Kachru, A. Klemm, W. Lerche, P. Mayr, and C. Vafa, "Nonperturbative results on the point particle limit of $N = 2$ heterotic string compactifications," Nucl Phys. **B459** (1996) 537–558, hep-th/9508155.

[9] A. Klemm, W. Lerche, P. Mayr, C. Vafa, and N. Warner, "Self-dual strings and $N = 2$ supersymmetric field theory," Nucl. Phys. **B477** (1996) 746–766, hep-th/9604034.

[10] W. Lerche and N. Warner, "Exceptional SW geometry from ALE fibrations," hep-th/9608183.

[11] A. Brandhuber and S. Stieberger, "Self-dual strings and stability of BPS states in $N = 2$ $SU(2)$ gauge theories," hep-th/9610053.

[12] A. Johansen, "A comment on BPS states in F-theory in 8 dimensions," hep-th/9608186.

[13] E. Martinec and N. Warner, "Integrable systems and supersymmetric gauge theory," Nucl. Phys. **B459** (1996) 97–112, hep-th/9509161.

[14] H. Itoyama and A. Morozov, "Prepotential and the Seiberg-Witten theory," hep-th/9512161.

[15] A. Gorsky, A. Marshakov, A. Mironov, and A. Morozov, "N=2 supersymmetric QCD and integrable spin chains: rational case $N_f < 2N_c$," Phys. Lett. **B380** (1996) 75–80, hep-th/9603140.

[16] S. Nam, "Integrable structure in SUSY gauge theories, and string duality," hep-th/9607223.

[17] A. Fayyazuddin, "Results in supersymmetric field theory from 3-brane probe in F-theory," hep-th/9701185.

[18] J. Schulze and N.P. Warner, "BPS geodesics in $N = 2$ supersymmetric Yang-Mills theory," hep-th/9702012.

[19] P. Henrici, *Applied and Computational Complex Analysis*, Vol. I, Wiley, New York 1974.

[20] A. Hanany and Y. Oz, "On the quantum moduli space of vacua of $N = 2$ supersymmetric $SU(N_c)$ gauge theories," Nucl. Phys. **B452** (1995) 283–312, hep-th/9505075.